RP Current Trends In Applied Sciences (e-ISSN: 2583-7486)
Vol. 5, No. 1 (January – March 2026) pp. 54–64

Cite this article: M. Aamir, M. Umair, M. Alam, S. Malik, Numerical investigation of blast-induced structural response of a bowstring steel girder bridge considering eccentric blast locations and supports, *RP Cur. Tr. Appl. Sci.* **5** (2026) 54–64.

Original Research Article

Numerical investigation of blast-induced structural response of a bowstring steel girder bridge considering eccentric blast locations and supports

Mohd Aamir[1], Mohammad Umair[1], Mehtab Alam[2], Sheela Malik[1]

[1]Department of Civil Engineering, Jamia Millia Islamia, New Delhi, 110025, India
[2]Department of Civil Engineering, Netaji Subhas University of Technology, West Delhi 110 073, India
*Corresponding author, E-mail: mohdaamirkhan1996@gmail.com

ARTICLE HISTORY
Received: 09 April 2026
Revised: 27 May 2026
Accepted: 27 May 2026
Published: 12 June 2026

KEYWORDS
Steel girder-bridge; Finite element analysis; Dynamic response; Johnson–Cook material model; Explosive loading.

ABSTRACT
This study examines the blast resistance behavior of a bowstring steel girder bridge under air-blast loading while accounting for realistic bearing constraint conditions. A thorough three-dimensional nonlinear finite element model of the bridge was produced using ABAQUS/Explicit (2017). The bridge system consists of steel deck plates, longitudinal girders, and transverse girders supported by pot bearings positioned on concrete support blocks. The structural steel components were modelled using the Johnson-Cook (J-C) plasticity and damage model to accurately capture strain rate effects under high-intensity loading. For a variety of detonation scenarios, including mid-span and end-span explosions, blast loads were applied under fixed and expansion bearing support conditions using the CONWEP blast loading model (CBLM). The structural response of the bridge was evaluated in terms of displacement behavior, stress distribution, and deformation patterns. The results demonstrate that vertical displacement is the most common reaction mode and that eccentric blast scenarios produce more asymmetric deformation and noticeable torsional effects than mid-span detonations. Furthermore, the study shows that realistic bearing constraint conditions have a significant impact on the deformation pattern and stress concentration within the bridge system. These findings highlight the importance of accurately modeling support circumstances for assessing the blast performance of steel bridge structures and provide insightful information for improving blast-resistant bridge designs.

1. Introduction

Bridges are important parts of the transportation system and are very important for making sure that people can move around quickly and that the economy grows. Strategically important bridges are subject to accidental explosions, terrorist strikes, and industrial blasts. These events can destroy buildings, disrupt services, and kill people. Because of this, understanding how bridges react structurally to blast stress has become a major area of research in structural and transportation engineering [1, 2]. Blast loads are defined by extremely high-pressure waves acting over a short period of time. These pressures induce a variety of complex dynamic responses in structures, including large displacements, high strain rates, and localized damage. Unlike conventional static, blast loads have the ability to significantly bend, shear, and twist bridge components [3, 4]. Steel bridges, particularly girder-type bridge systems, may experience significant deformation and stress concentration when subjected to blast loads [5].

Steel girder bridges are popular due to their structural efficiency and ability to withstand huge loads with a small profile. Deck components and longitudinal and transverse girders distribute loads on these bridges. Under severe dynamic stresses like explosions, these components may interact to cause complex deformation patterns and structural collapse [6]. Advancements in computational techniques have made finite element analysis a powerful tool for analyzing how bridge structures respond to high loading conditions. Numerical modeling allows researchers to explain complex structural systems and capture nonlinear material behavior under dynamic pressures. Finite element software such as ABAQUS has been widely used for blast studies of bridge structures because it can predict high-strain-rate material behavior and rapid dynamic loads [7, 8]. Blast loads cause structural steel, strain-rate effects, and plastic deformation. The Johnson-Cook (C-J) constitutive model is used in blast and impact simulations to accurately portray metallic material strain hardening, strain-rate sensitivity, and thermal softening [9, 10]. Predicting bridge system structural reaction needs material modeling and support conditions. Bridges often use pot bearings and other bearing systems to transfer loads from the superstructure to the substructure while allowing controlled translation and rotation. Many computer studies oversimplify support conditions and ignore the effect of true bearing constraints on bridge structural reaction under blast pressure [11]. Another factor determining blast reaction is the explosion position relative to the bridge span. Explosions near the supports or end-span portions might induce torsional effects and uneven stress distribution, whereas mid-span blasts normally cause symmetric deformation patterns [12].

Recent research has focused on steel box girder bridges and composite bridge systems, which are common in modern bridge building. Recent computer studies on far-field blast-loaded steel box girder bridges indicated that explosion intensity and stand-off distance considerably affect dynamic response and damage patterns [7-10]. Parametric studies on box girder bridges show that geometry and layout considerably affect blast resistance and deformation [11]. High-explosive charges can damage bridge decking and girders, especially around mid-span portions with considerable bending loads, according to experimental and numerical studies [32].

Thus, blast location and bearing restraint circumstances must be studied to understand steel bridge system dynamics. An extensive three-dimensional finite element model of a bowstring steel girder bridge is created to analyze its structural reaction to blast loads. The bridge is supported by pot bearings over concrete blocks and studied under several configurations. CONWEP blast loading applies mid- and end-span blast loads. The bridge's displacement behavior, stress distribution, torsional effects, support reactions, and damage patterns are assessed. Understanding steel bridge system dynamics requires studying blast location and bearing restraint. A thorough three-dimensional finite element model of a bowstring steel girder bridge analyzes blast load response. The bridge is supported by pot bearings over concrete blocks and studied in several configurations. CONWEP blasts mid-span and eccentric end-span locations. Assessments include bridge displacement, stress distribution, torsional effects, support reactions, and damage patterns.

2. Literature review

2.1 Blast effects on structural systems

Blast loading consists of a high-intensity positive pressure phase followed by a negative suction phase. This creates strong impulsive forces and dynamic amplification effects on structures. Initial research predominantly concentrated on protective systems and reinforced concrete components. Hao and Tang [1] conducted a numerical analysis of the response of cable-stayed bridge components to explosive loading, revealing that flexural and shear failures predominate in pier and deck systems. Hashemi et al. [41] established that the location of detonation markedly affects displacement amplification and progressive damage in long-span bridge structures. In the same way, Pan et al. [25] found that explosions below the deck cause more damage than those above the deck because of the effects of confined pressure.

These studies collectively demonstrate that structural vulnerability under blast loading is significantly influenced by parameters such as charge weight, stand-off distance, and explosion location. Nevertheless, the majority of studies are confined to simplified structural configurations.

2.2 Effect of blast loading on steel bridges

Recent studies have concentrated on the response of steel girder bridges to blast loading, given their prevalent utilization. Zhang et al. [48] examined the dynamic response of steel box girder bridges subjected to far-field blast loading and identified stress concentration near supports as a pivotal factor affecting global stability. The research additionally suggested damage indices for the assessment of structural performance. Lei Zhang et al. [34] utilized a coupled CFD–explicit dynamics methodology to precisely simulate blast wave diffraction and pressure distribution. Their probabilistic assessment showed that the more intense the blast, the worse the damage. On the other hand, the higher the incidence angle, the less likely the pier is to fail. Xie et al. [10] performed structural optimization studies, illustrating that geometric alterations can markedly diminish peak displacement and stress demand.

These improvements, most studies still use idealized boundary conditions and don't include detailed modeling of bearing systems. This could make the predicted structural responses less accurate.

2.3 Effects of explosions on concrete girder bridges

Researchers have also looked at concrete girder bridges a lot when they are subjected to blast loading. Tian et al. [7] examined simply supported concrete girder bridges under extensive blast conditions and found that mid-span areas are especially vulnerable to flexural cracking and cumulative damage. The research highlighted the impact of augmented charge weight on crack propagation and structural deterioration.

However, existing research primarily focuses on global structural response, with limited attention to localized damage mechanisms and component interaction.

2.4 Influence of support and bearing conditions

Structural dynamic response relies heavily on supporting factors. The redistribution of forces, the acceleration of stress near supports, and the torsional rotation are all impacted by the stiffness of the restraints when subjected to impulsive loading. Bridge supports are typically considered fixed or supported boundary conditions in finite element studies. Pot bearings provide for the rotation and translation of bridge superstructures. A blast's dynamic response can be significantly altered by the use of guided, expansion, or fixed bearings. Research on blast analysis of girder bridges that specifically models bearing systems is limited.

Detailed numerical research on blast-loaded bowstring girder bridges is needed, including realistic support models and composite deck interaction.

3. Research gap and objectives

Based on the reviewed literature, the following important research gaps are identified:

- Most research focuses on Cable Stayed Bridge and Box Girder Bridge, but Composite Bowstring Girder Bridge under blast stress is rarely examined.
- In explosion analysis, realistic pot-bearing behavior is frequently disregarded.
- The steel–concrete interface behavior under blast loading has limited scientific coverage.
- There aren't enough thorough frameworks for evaluating damage to composite bowstring bridges.

In light of the identified gaps, the primary objectives of this study are:

- Using ABAQUS, create a three-dimensional nonlinear finite element model of a girder bridge under blast loading.
- Realistic pot-bearing systems with expansion and fixed support conditions can be simulated.
- To apply material nonlinearities, use the Johnson-Cook Model for steel and the Concrete Damage Plasticity Model for concrete.
- Examine the impact of blast characteristics like eccentric detonation locations and charge weight.

- Use displacement, stress distribution, and damage indices to assess the structural reaction.

4. Numerical modeling

4.1 Finite element modeling of the bridge

For this study, we chose a conventional bowstring steel girder bridge and used the explicit dynamic solver in the finite element software ABAQUS (2017) to model it. This study examined a highway infrastructure-style simply supported bridge with a 46.32-m span. The bridge deck has two 7.35-m-wide traffic lanes and a load-carrying framework of longitudinal and transverse steel girders. The bridge superstructure consists of eight 5.49-m-long structural panels that comprise the span. The bridge's bowstring arch rises to 9 m at the mid-span, giving it its distinctive look.

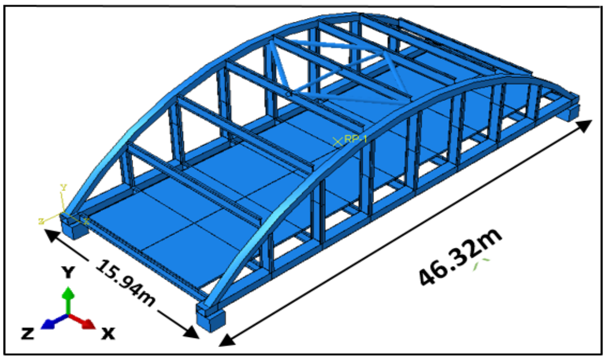

(a) Isometric view of the steel bridge

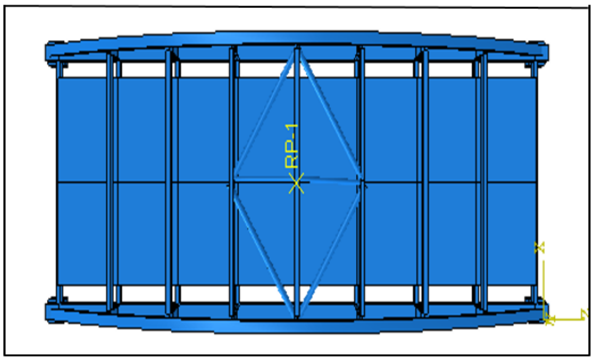

(b) top view of the steel bridge

Figure 1: Isometric and top views of the bowstring steel girder bridge.

The steel girder structure is supported by pot bearings over concrete support blocks, mimicking bridge support. The numerical model considers fixed and expansion support border designs. To accurately describe structural behavior under blast loading, the finite element model was discretized using eight-node reduced integration brick elements (C3D8R). Near bearings and connecting zones, a revised mesh was used to account for large stress gradients. Advanced constitutive models for structural components simulated material behavior under high-strain-rate loading. The mechanical parameters of structural steel include a Young's modulus of 210 GPa, a density of 7850 kg/m³, and a Poisson's ratio of 0.30. The Johnson–Cook plasticity and damage model studied steel plasticity under blast loading, including strain hardening and strain-rate dependent behavior. The CONWEP blast loading approach provides pressure–time histories from TNT equivalent explosive charges. It simulates air-blast effects on structural systems realistically and is commonly used in blast-resistant structural analysis.

4.2 Material modeling

Predicting bridge structural reaction to blast loading requires accurate material behavior characterization. High-strain-rate circumstances can cause plastic deformation, strain-rate sensitivity, and gradual deterioration in structural materials. To simulate bridge component behavior, the finite element model used appropriate constitutive models. This study's bridge structure is mostly structural steel members, such as longitudinal, transverse, and bearing plates on concrete blocks. Multiple material models were used to mimic steel and concrete components under blast loading.

4.2.1 Steel material properties

Bridge steel components were modeled using an elastic–plastic material model and strain-rate dependent constitutive relations. Common bridge steel parameters were used to determine structural steel properties. Steel's elastic properties include a density of 7850 kg/m³, a Poisson's ratio of 0.30, and a Young's modulus of 210 GPa. In addition to elastic behavior, plastic deformation was used to describe yielding and strain hardening. The structure steel yield strength was estimated at 355 MPa, and ultimate strength was 510 MPa, which is compatible with bridge construction grades.

4.2.2 Johnson–Cook Plasticity Model

The Johnson–Cook plasticity model was used in finite element analysis to steel's high-strain-rate behavior under blast stress. This constitutive model accounts for strain hardening, strain-rate sensitivity, and thermal softening in metallic materials, making it popular in blast and impact simulations. The Johnson–Cook model calculates flow stress from plastic strain, strain rate, and temperature. In this work, blast analysis literature values for structural steel were used to select model parameters. The yield stress parameter (A) was 355 MPa, the hardening modulus (B) was 510 MPa, and the strain hardening exponent (n) was 0.67. We assumed a 0.014 strain-rate sensitivity constant (C) and a 1.0 thermal softening exponent (m). A reference strain rate of 1 s^{-1} was used, with room and melting temperatures of 20°C and 1500°C, respectively.

4.2.3 Johnson–Cook Damage Model

In addition to plastic deformation, the Johnson–Cook damage model analyzed blast-loaded structural collapse. This model shows how plastic strain and strain-rate effects cause and evolve metallic material damage. The damage parameters used in this investigation are D1 = 0.05, D2 = 3.44, D3 = 2.12, D4 = 0.002, D5 = 0.61, and melting temperature = 1500°C. These parameters allow the finite element model to predict steel component degradation and failure under high-intensity blast loads.

4.2.4 Concrete Block Modeling

A bridge support system uses concrete blocks as pot-bearing seats. To simulate dynamic loading, these concrete components were modeled using nonlinear material behavior. Concrete cracking and crushing were simulated using the

Concrete Damage Plasticity model. This model can simulate tensile cracking and compressive failure stiffness degradation. This material model simulates concrete support block behavior under blast-induced dynamic loads carried through the bearing system.

4.3 Bearing modeling

Bearings help bridge constructions transfer loads from the superstructure to the substructure while absorbing thermal expansion, traffic loads, and dynamic impacts. This work models the bridge support system employing pot bearings on concrete support blocks to approximate genuine bridge boundary conditions. The numerical model considers fixed and expanding bearing restrictions, as shown in Fig. 2. The fixed bearing stops rotation at the support position and movement in all horizontal directions, which makes the structure stiffer and less likely to shift. The expansion bearing lets the bridge span move along its length but not up or down. This lets the bridge deck expand or contract while it is under load. The ABAQUS finite element model uses boundary restrictions at the bearing nodes to mimic these bearing conditions. The fixed bearing limits the degrees of freedom for moving along the length and width of the structure, whereas the expansion bearing allows movement along the length but limits vertical movement to keep the structure stable.

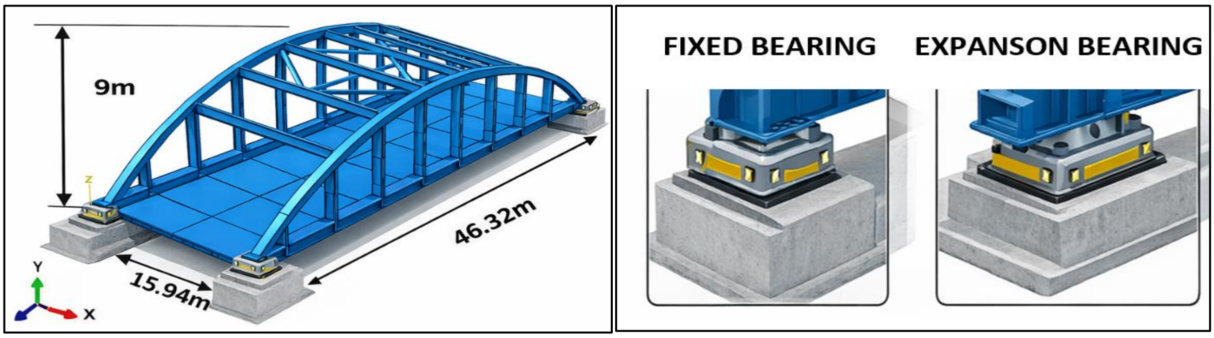

Figure 2: Diagrammatic depiction of the fixed and expansion bearing support conditions for steel bridges.

4.4 Mesh modeling and boundary conditions

Three-dimensional solid elements in ABAQUS discretized bridge components. Different mesh sizes were used for structural components to balance computational accuracy and efficiency. The steel girders were modeled with mesh sizes ranging from 50–100 mm, while the pot bearing components were discretized using a finer mesh size of 20–40 mm to capture localized stress concentrations. The concrete support blocks were modeled with mesh sizes between 75–150 mm. The selected mesh configuration ensures stable numerical results and accurate representation of stress wave propagation during blast loading, as shown in Fig. 3.

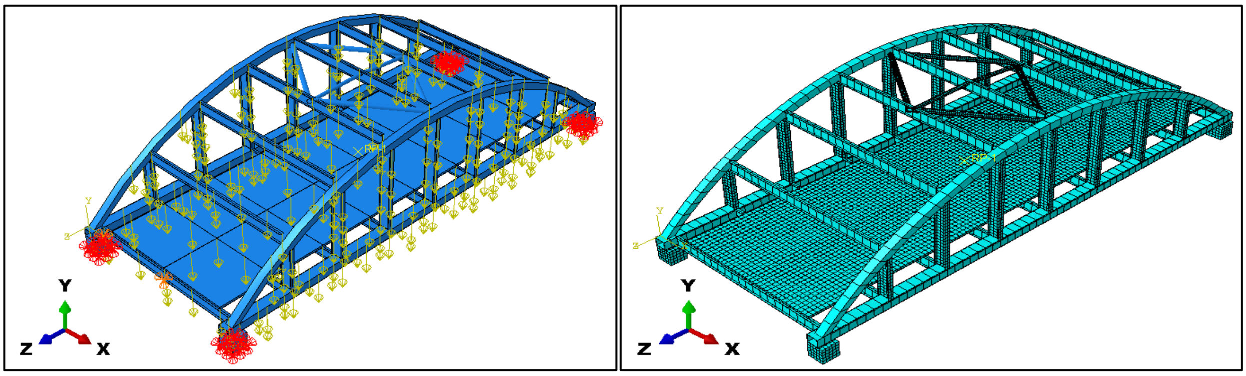

Figure 3: Finite element mesh and boundary conditions of the steel bridge model.

Realistic bridge support behavior was represented by simple support boundary conditions. Concrete support blocks held fixed, and expansion pot bearings for the bridge. The fixed bearing restrained horizontal displacements, while the expansion bearing allowed longitudinal movement of the bridge to simulate realistic expansion behavior. The dynamic response of the structure under blast loading was analyzed using the explicit solver in ABAQUS/Explicit.

4.5 Bowstring steel bridge effect blast loading

This study uses the ABAQUS code [21], Figure 1, to model a conventional Bowstring steel girder bridge with a span length of 46.32 m (Fig. 1). The model bridge is thought to have two 7.35 m lanes. There are eight panels on the bridge, and each one is 5.49 m long. The overall height of the arches at mid-span is 9 m.

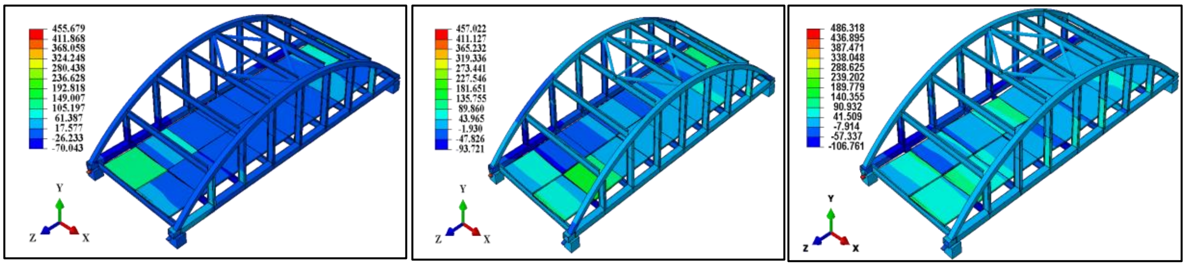

(a) Mid-span Eccentric 500kg TNT (b) Mid-span Eccentric 100kg TNT (c) Mid-span Eccentric 1500kg TNT

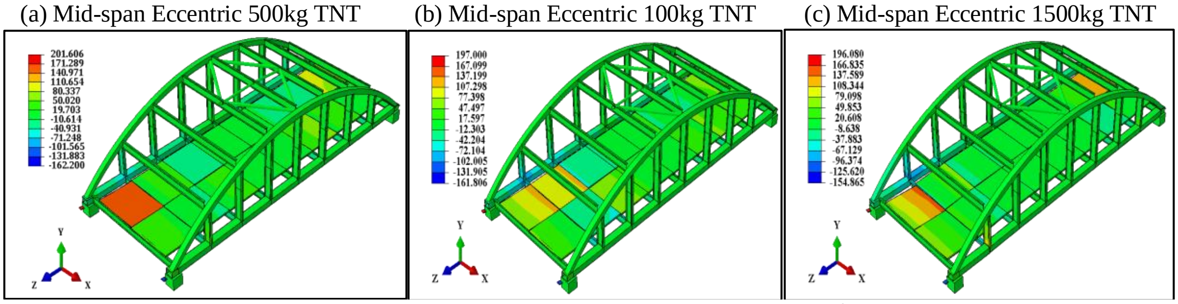

(d) End-span Eccentric 500kg TNT (e) End-span Eccentric 1000kg TNT (f) End-span Eccentric 1500kg TNT

Figure 4: The Bridge Models X-displacement (mm) Profiles.

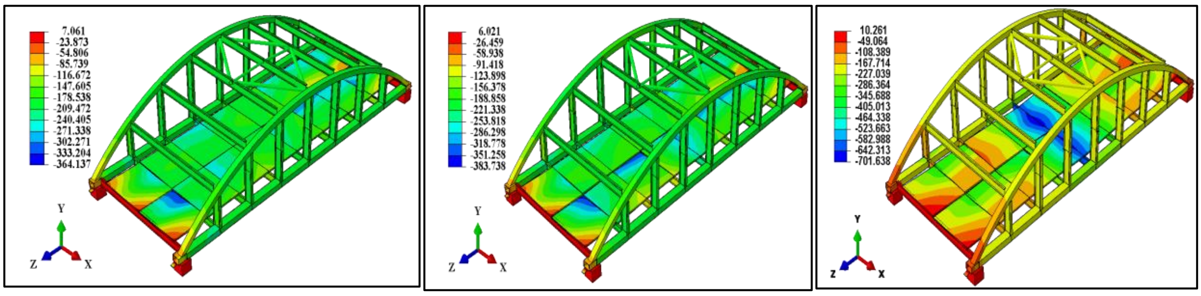

(a) Mid-span Eccentric 500kg TNT (b) Mid-span Eccentric 100kg TNT (c) Mid-span Eccentric 1500kg TNT

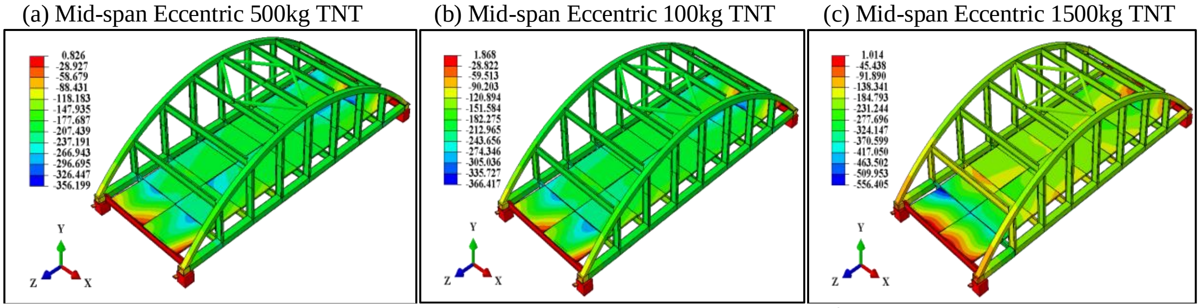

(d) End-span Eccentric 500kg TNT (e) End-span Eccentric 100kg TNT (f) End-span Eccentric 1500kg TNT

Figure 5: The Bridge Models Y-displacement (mm) Profiles.

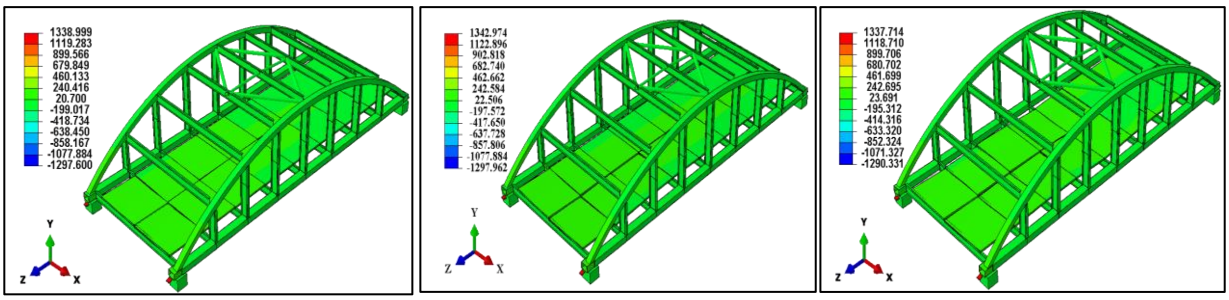

(a) Mid-span Eccentric 500kg TNT (b) Mid-span Eccentric 100kg TNT (c) Mid-span Eccentric 1500kg TNT

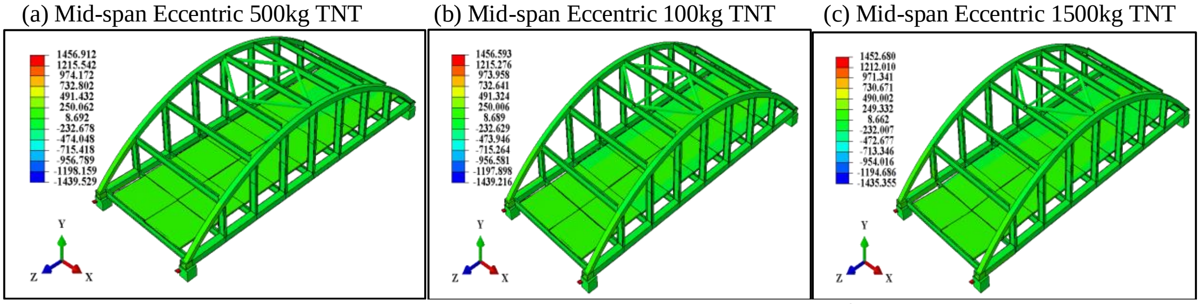

(d) End-span Eccentric 500kg TNT (e) End-span Eccentric 100kg TNT (f) End-span Eccentric 1500kg TNT

Figure 6: The Bridge Models Z-displacement (mm) Profiles.

The model is discretized with C3D8R elements. Strain-rate effects on steel are accounted for when using the UFC 3–340-02(2008) [22, 24] design code for the blast analysis of structures. The plastic behavior of the steel has been described using the Johnson-Cook damage plasticity model in ABAQUS. The model's parameters are derived from the literature [1–18, 22–28]. The bridge is modeled using ABAQUS's default interactions, restrictions, and boundary conditions [21].

Blast load: An explosion is a quick release of energy into the air that creates a blast wave. There are numerous kinds of explosions, such as physical, chemical, and nuclear explosions. Chemical explosions are the most prevalent type of explosion that can happen by accident or as a result of a terrorist assault [22–26]. The blast characteristics describe a temporary pulse of pressure that quickly spreads out from the site of the explosion. The first step in designing or analyzing a blast is to figure out how much force it will have [2–36]. Blasts can create very intense and extreme loads. Even a small amount of explosives can wreak a lot of harm to a building if they are put in the right places [15]. Explosions can put pressures on structures that are many times higher than the normal design loads. Dynamic pressure may still cause drag stresses on the rest of the structural frame. If there is an explosion on top of the bridge, the girders and deck slab that hold it up are pushed down by the overpressure [16]. Calculating the equivalent load from a blast explosion is a difficult task. The blast pressure gets weaker the farther away you are from the center of the explosion.

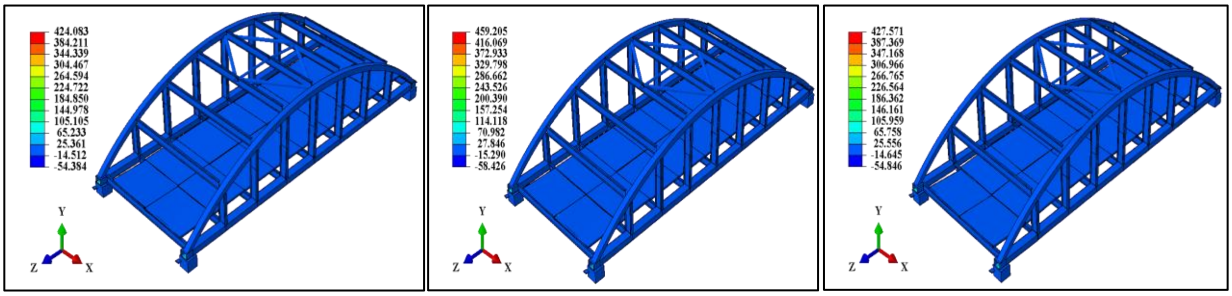

(a) End-span Eccentric 500kg TNT (b) End-span Eccentric 100kg TNT (c) End-span Eccentric 1500kg TNT

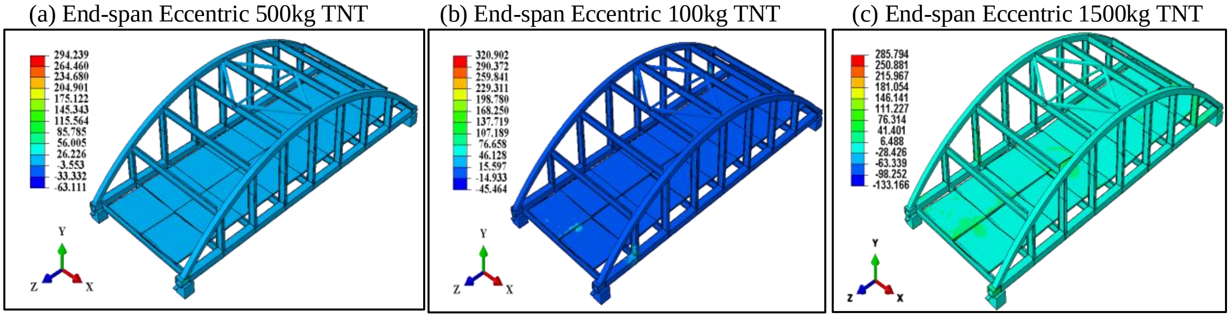

(d) Mid-span Eccentric 500kg TNT (e) Mid-span Eccentric 100kg TNT (f) Mid-span Eccentric 1500kg TNT

Figure 7: Maximum principal stress (MPa) profiles (Positive values indicate tensile).

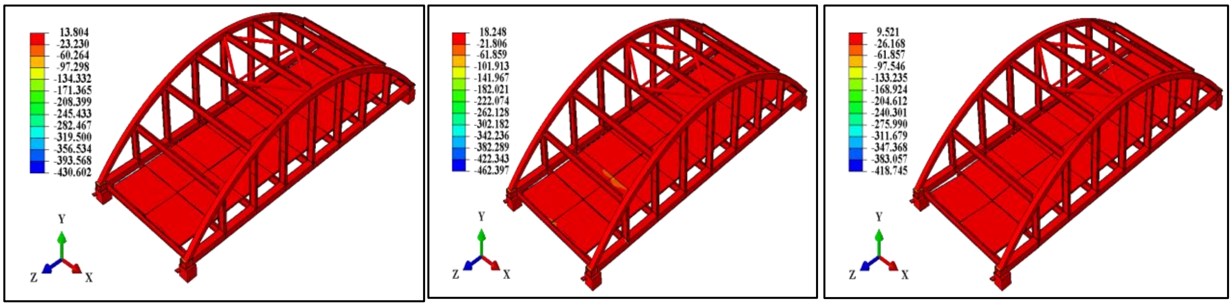

(a) End-span Eccentric 500kg TNT (b) End-span Eccentric 100kg TNT (c) End-span Eccentric 1500kg TNT

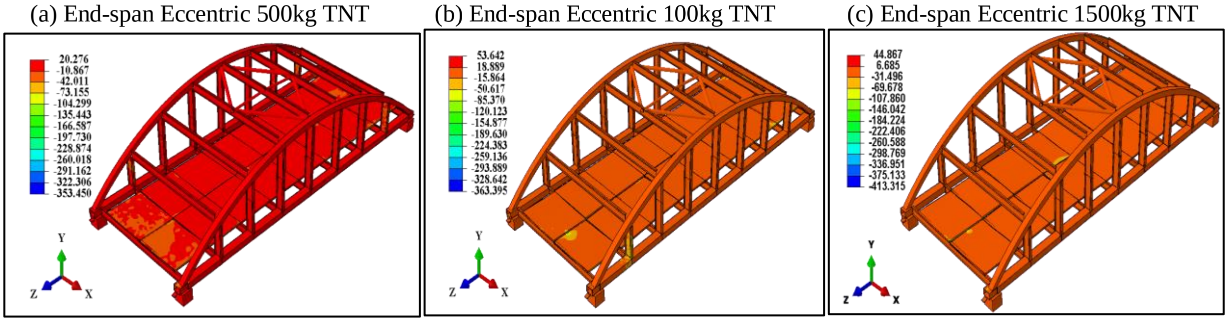

(d) Mid-span Eccentric 500kg TNT (e) Mid-span Eccentric 100kg TNT (f) Mid-span Eccentric 1500kg TNT

Figure 8: Minimum principal stress (MPa) profiles (Positive values indicate tensile).

The CONWEP method, which uses empirical relationships from UFC 3-340-02 (2008) to estimate air-blast pressure, is used in ABAQUS to simulate blast loading. The TNT-equivalent approach is used to model the explosive charge and the scaled distance. The blast pressure of an explosion is inversely proportional to the scaled distance, as shown in Eq. (1).

$$Z = \frac{R}{W^{\frac{1}{3}}}$$

where W is the TNT equivalent mass and R = the target's distance (m) from the explosion's point, it is used to determine the blast severity. Two explosion locations, mid-span and end-span, are taken into consideration for three charge weights (500 kg, 1000 kg, and 1500 kg TNT).

Blast load and its profile with time are calculated using Wu and Hao's (2005) [24] blast model, which is based on a number of empirical equations and the Con-WEP 2.0 semi-empirical technique in [21]. The explosion locations taken into consideration in this work include near support, mid-span, and end-span. ABAQUS computer code is used to create a total of six finite element models of the bridge. Three alternative intensities of explosions are evaluated near the middle of the deck in these areas, as well as the lateral eccentricity of quarter deck width corresponding to these locations. For this analysis, large explosive loads of 500 kg, 1000 kg, and 5000 kg-TNT at a constant stand-off distance of 1.0 m above the deck slab are taken into consideration. The reference point keycard in ABAQUS is used to apply the charge in the free-air environment.

5. Results and discussion

The results of the analysis show the blast loadings of explosive charges of 500 kg, 1000 kg, and 1500 kg-TNT in eccentric places on 60 mm thick steel plates of the steel bridge deck without a concrete slab. The potential explosion that occurred during construction before the bridge was opened to traffic is reflected in this analysis. This work cannot accommodate the simulation of the bridge with the concrete deck slab on the steel plates, its outcomes, and comparisons.

The following observations are notable from the blast analysis conducted:

5.1 Locations of eccentric explosives

The displacement response of the bowstring steel girder bridge subjected to blast loading is summarized in Table 1, while the displacement contours in the X-, Y-, and Z-directions are illustrated in Fig. 4–6. The structural response was evaluated for both mid-span (MS) and end-span (ES) blast scenarios with different explosive masses.

Table 1: Bridge's displacement response (all displacement values are considered ve).

Figures	Model ID	Maximum Displacement of X, Y, and Z (mm) in different Components near the area of concern for the explosion		
		Steel Plate	Transverse Girder	Longitudinal Girder
Fig. 4-(a)	MS-E-500	70.043	26.233	17.577
Fig. 4-(b)	MS-E-1000	93.721	47.826	19.130
Fig. 4-(c)	MS-E-1500	106.761	57.337	27.914
Fig. 4-(d)	ES-E-500	162.200	131.883	102.005
Fig. 4-(e)	ES-E-1000	161.802	131.905	102.005
Fig. 4-(f)	ES-E-1500	154.137	125.620	96.374
Fig. 5-(a)	MS-E-500	364.137	333.204	302.271
Fig. 5-(b)	MS-E-1000	383.738	351.258	318.778
Fig. 5-(c)	MS-E-1500	701.638	642.310	582.988
Fig. 5-(d)	ES-E-500	356.199	326.447	296.695
Fig. 5-(e)	ES-E-1000	366.417	335.727	305.036
Fig. 5-(f)	ES-E-1500	556.405	509.953	463.502
Fig. 6-(a)	MS-E-500	1297.600	1077.884	858.167
Fig. 6-(b)	MS-E-1000	1297.962	1077.884	857.806
Fig. 6-(c)	MS-E-1500	1290.331	1071.327	852.324
Fig. 6-(d)	ES-E-500	1439.529	1198.159	956.789
Fig. 6-(e)	ES-E-100	1439.216	1197.898	956.581
Fig. 6-(f)	ES-E-1500	1435.355	1194.686	954.016

- The longitudinal girder of the deck experiences a maximum X-displacement of 17.577 mm as a result of a mid-span eccentric 500 kg explosion (Fig. 4-(a)). The X-displacement reduces as the explosive charge location shifts from mid-span to near supports, Fig. 4.
- Bridge component deformation along the Y-direction is depicted in the transverse displacement response shown in Fig. 5-(d). 296.695 mm is the maximum displacement. This displacement in the longitudinal girder under the ES-E-500 explosion scenario shows that asymmetric loading circumstances caused by eccentric blast loading result in severe transverse deformation.
- The vertical displacement contours in Fig. 6 (c) indicate how the bridge structure bends the most. The results demonstrate that eccentric blast loading causes the most vertical movement, with the longitudinal girder moving about 852.324 mm at its most. This shows that unequal blast loading can greatly increase the bending deformation of the bridge structure.
- The stress study shows that the highest primary stress is about 459.205 MPa, and the lowest principal stress is 9.521 MPa. The most stress is concentrated in the connectors and support areas of the girders, which shows how weak these parts are when they are hit by a bomb.

- The bridge structure bends up and down because the mid-span blast loading causes it to deform in a rather symmetrical way. Eccentric end-span blast loading causes the girders to clearly twist because it puts pressure on them unevenly. The results show that eccentric explosions make torsional effects much worse, making structures more likely to fail near supports and connections.

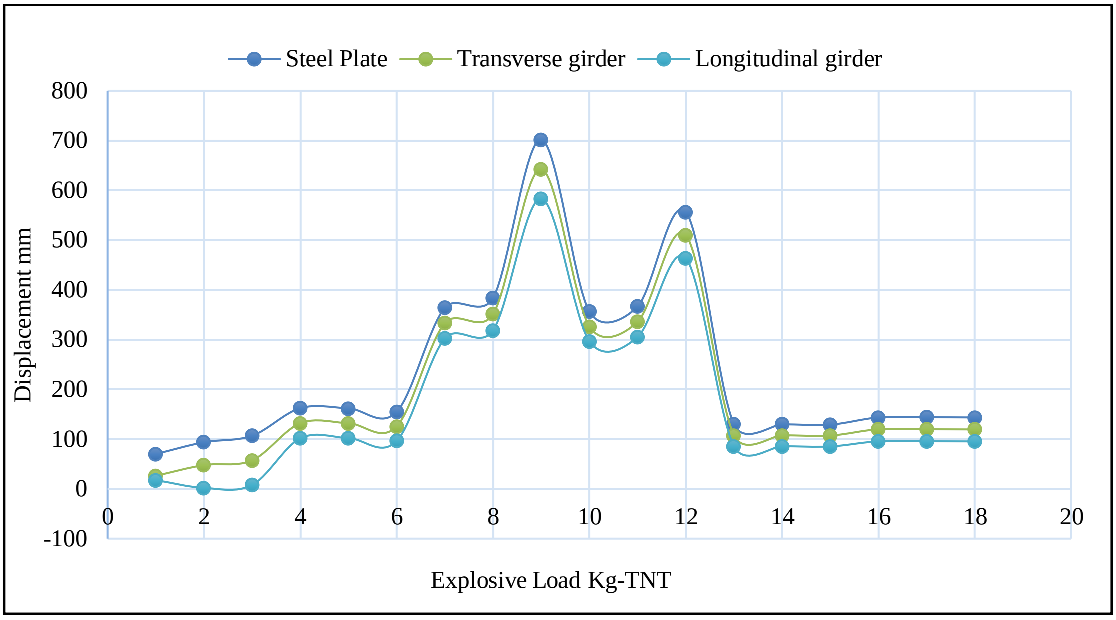

Figure 9: Responses of steel plate, transverse, and longitudinal girder under different masses of explosive charges.

The displacement responses of the bridge components under various blast loads are compared in Figure 9. The results demonstrate that displacement typically increases with increasing explosive charge mass, highlighting the load transfer behavior within the bridge structural system. The longitudinal and transverse girders experience the least amount of distortion after the steel plate.

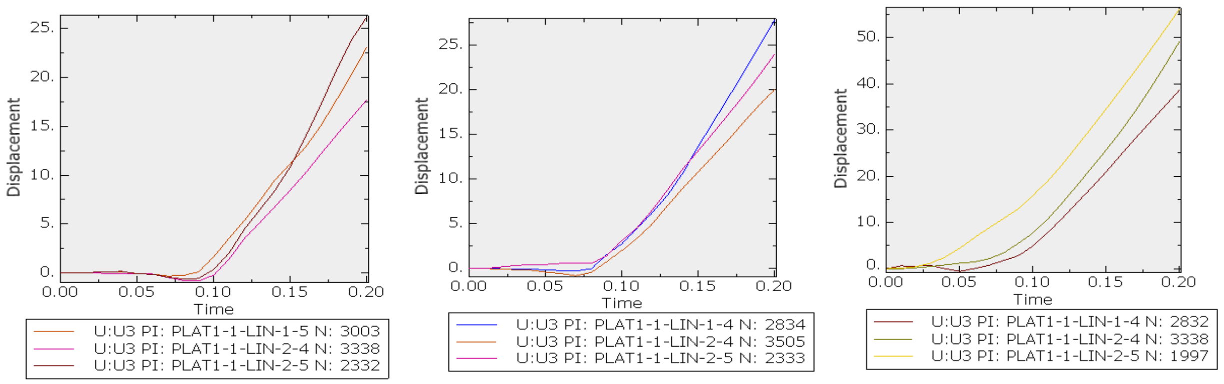

(a) MS-E-500 (b) MS-E-1000 (c) MS- E-1500

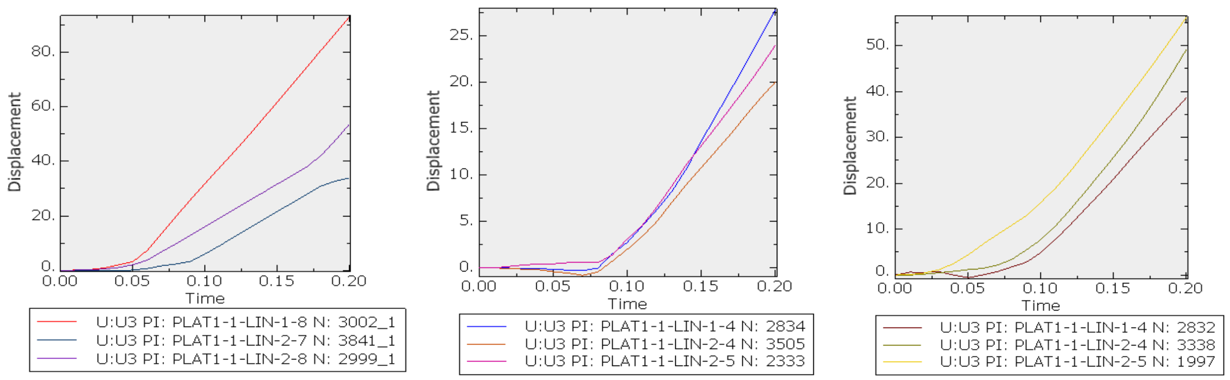

(a) ES-E-500 (b) ES-E-1000 (c) ES- E-1500

Figure 10: Time-history response of vertical displacement (U3) at selected bridge (Plate) nodes.

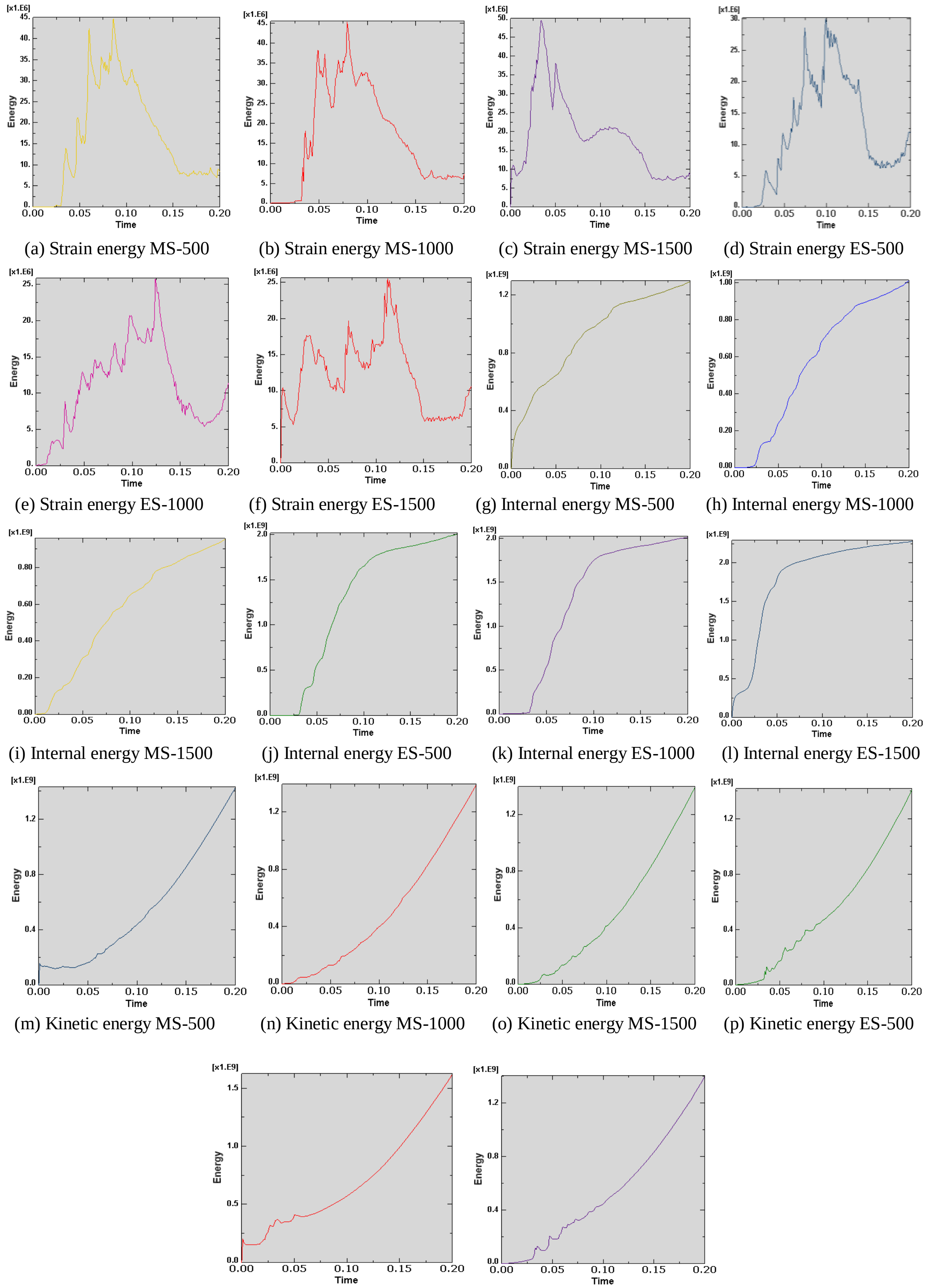

(a) Strain energy MS-500 (b) Strain energy MS-1000 (c) Strain energy MS-1500 (d) Strain energy ES-500

(e) Strain energy ES-1000 (f) Strain energy ES-1500 (g) Internal energy MS-500 (h) Internal energy MS-1000

(i) Internal energy MS-1500 (j) Internal energy ES-500 (k) Internal energy ES-1000 (l) Internal energy ES-1500

(m) Kinetic energy MS-500 (n) Kinetic energy MS-1000 (o) Kinetic energy MS-1500 (p) Kinetic energy ES-500

(q) Internal energy ES-1000 (r) Internal energy ES-1500

Figure 11: Energy – time histories of the bridge under blast loading at mid-span and end-span for explosive masses of 500kg, 1000kg, and 1500kg TNT.

- Figure 10. The variation of vertical displacement (U3) with time at selected nodes of the bridge subjected to blast loading. The displacement remains small during the initial stage and increases rapidly after approximately 0.08–0.10 s due to the impulsive blast pressure. The curves indicate significant dynamic deformation and vibration of the bridge system, with peak displacement occurring at later stages of the response.

Energy–Time Response of the Bridge under Blast Loading

- The energy–time histories illustrate the evolution of strain energy, internal energy, and kinetic energy of the bridge subjected to blast loads of 500 kg, 1000 kg, and 1500 kg TNT at the mid-span (MS) and end-span (ES) locations shown in Figure 11.
- After the explosion, the strain energy rises quickly, showing that the blast pressure generated a lot of structural deformation. More powerful explosives create higher peak strain energy values, which means that the bridge parts are more likely to break and get damaged.
- The internal energy rises steadily throughout the course of the simulation, which depicts how the structural system gradually absorbs energy from the blast. The findings reveal that increased charge masses result in heightened energy accumulation, illustrating the significant correlation between structural reaction and explosion intensity.
- The kinetic energy curves show how the blast wave causes things to move. For all charge masses, the kinetic energy trend is rising, which means that the energy from the blast is being transferred to structural vibration and inertia effects.

6. Conclusions

This study numerically investigates the dynamic response of steel girder bridge subjected to blast loading using nonlinear finite element analysis in ABAQUS.

The following conclusions can be made based on the numbers:

- The bridge's displacement reaction rises as the explosive mass increases, suggesting that structural deformation is greatly increased by higher explosion intensity.
- Eccentric end-span blast loading causes higher deformation and torsional effects than mid-span explosions due to asymmetric blast pressure distribution.
- According to stress analysis, significant stress concentrations are found close to girder connections and support areas, with the maximum principal stress reaching roughly 459 MPa.
- The energy-time histories demonstrate that blast energy is initially transformed into kinetic energy, subsequently dissipated through strain and internal energy, confirming the dynamic energy transfer mechanisms within the bridge structure.

In general, the results show how important it is to think about the size of the explosive charge, the position of the blast, and realistic support circumstances when designing and testing blast-resistant steel bridge systems. Adding these aspects is necessary to precisely estimate how a structure would respond and to make bridge constructions more resilient and safer in case of an explosion.

Authors' contributions

The author read and approved the final manuscript.

Conflicts of interest

The author declares no conflict of interest.

Funding

This research received no external funding.

Data availability

No new data were created.

References

[1] H. Hao, C. Wu, G. Ma, Z. Chen, Numerical simulation of a cable-stayed bridge response to blast loads, *Eng. Struct*. **32** (2010) 3180–3192.
[2] M. Talaat, E. Yehia, S.A. Mazek, M.M. Genidi, A.G. Sherif, Finite element analysis of RC buildings subjected to blast loading, *Ain Shams Eng. J*. **13** (2022) 101689.
[3] J.C. Gannon, K.A. Marchand, E.B. Williamson, Approximation of blast loading and single degree-of-freedom modelling parameters for long span girders, (2006).
[4] ABAQUS/CAE FEA Program, Arch bridge model, blast loading mid-span, quarter span, and end-span, ABAQUS DS-SIMULIA User Manual (2017).
[5] H. Hao, Z. Li, Numerical study of structural response of bridges subjected to blast loads, *Eng. Struct*. (2011).
[6] A. Alsendi, C.D. Eamon, Reliability of steel girder bridges subjected to blast loads, *ASCE-ASME J. Risk Uncertain. Eng. Syst. Part A Civ. Eng*. **11** (2025) 04024087.
[7] J. Tian, S. Cheng, Z. Liao, W. Yin, L. Ma, X. Sun, W. Liu, Dynamic response and failure analysis of concrete simply-supported girder bridges subjected to far-field large-scale equivalent blast loads, *Struct*. **79** (2025) 109624.
[8] C. Xie, H. Jin, Y. Xu, X. He, J. Zhou, Dynamic response and design optimization of box girder bridge with corrugated steel webs subjected to blast loads, *Infrastructures* **10** (2025) 256.
[9] M. Aamir, M. Alam, S.M. Anas, Effect of blast location and explosive mass on the dynamic behavior of a bowstring steel highway girder bridge subjected to an air-blast, *Mater. Today Proc*. **87** (2023) 20–29.
[10] S.M. Anas, M. Alam, M. Umair, Performance of one-way composite reinforced concrete slabs under explosive-induced blast loading, *IOP Conf. Ser.: Earth Environ. Sci*. **614** (2020) 012094.
[11] S.M. Anas, M.I. Ansari, M. Alam, Performance of masonry heritage building under air-blast pressure without and with ground shock, *Aust. J. Struct. Eng*. **21** (2020) 329–344.
[12] S.M. Anas, M.I. Ansari, M. Alam, A study on existing masonry heritage building to explosive-induced blast loading and its response, *Int. J. Struct. Eng*. **11** (2021) 387–412.
[13] S.M. Anas, M. Alam, M. Umair, Experimental and numerical investigations on performance of reinforced concrete slabs under explosive-induced air-blast loading: a state-of-the-art review, *Struct*. **31** (2021) 428–461.
[14] S.M. Anas, M. Alam, Comparison of existing empirical equations for blast peak positive overpressure from spherical free air and hemispherical surface bursts, *Iran. J. Sci. Technol. Trans. Civ. Eng*. **46** (2021) 965–984.
[15] S.M. Anas, M. Alam, M. Umair, Performance of on-ground double-roof RCC shelter with energy absorption layers under close-in air-blast loading, *Asian J. Civ. Eng*. **22** (2021) 1525–1549.
[16] S.M. Anas, M. Alam, M. Umair, Air-blast and ground shockwave parameters, shallow underground blasting, on the ground and buried shallow underground blast-resistant shelters: a review, *Int. J. Protect. Struct*. **13** (2021) 99–139.
[17] S.M. Anas, M. Alam, M. Umair, Out-of-plane response of clay brick unreinforced and strengthened masonry walls under explosive-induced airblast loading, in: S. Kolathayar, C. Ghosh, B.R. Adhikari, I. Pal, A. Mondal (Eds.), Resilient Infrastructure, Lect. Notes Civ. Eng., vol. 202, Springer, Singapore (2021) pp. 477–491.

[18] W.F. Cofer, D.S. Matthews, D.I. McLean, Effects of blast loading on prestressed girder bridges, *Shock Vib*. **19** (2012) 1–18.
[19] ABAQUS/CAE FEA Program Version 6.15, Concrete Damage Plasticity model, explicit solver, three-dimensional solid element library, interactions, restraints, keycard library, ABAQUS DS-SIMULIA User Manual, France.
[20] UFC 3-340-02, Structures to Resist the Effects of Accidental Explosions, Unified Facilities Criteria, U.S. Army Corps of Engineers (2008).
[21] C. Wu, H. Hao, Modeling of simultaneous ground shock and airblast pressure on nearby structures from surface explosions, *Int. J. Impact Eng*. **31** (2005) 699–717.
[22] S.M. Anas, M. Alam, M. Umair, Performance prediction of braced unreinforced and strengthened clay brick masonry walls under close-range explosion through numerical modelling, *Int. J. Comput. Mater. Sci. Surf. Eng*. **11** (2022) 120–146.
[23] M. Shariq, S.M. Anas, M. Alam, Blast resistance prediction of clay brick masonry wall strengthened with steel wire mesh, and C-FRP laminate under explosion loading: a finite element analysis, *Int. J. Reliab. Saf*. **16** (2022) 27–45.
[24] E. Maiorana, C.D. Tetougueni, P. Zampieri, Effect of blast load on the structural integrity of the steel arch bridge slab, *Eng. Fail. Anal*. **139** (2022) 106498.
[25] Y. Pan, C.E. Ventura, M.M. Cheung, Performance of highway bridges subjected to blast loads, *Eng. Struct*. **151** (2017) 788–801.
[26] L.L. Ma, H. Wu, Q. Fang, Damage mode and dynamic response of RC girder bridge under explosions, *Eng. Struct*. **243** (2021) 112676.
[27] H. Jia, H. Wei, J. Li, S. Cui, L. Xu, S. Zheng, Blast resistance of steel jacket reinforced double-column bridge pier, *Eng. Struct*. **329** (2025) 119882.
[28] S. Saha, S. Karmakar, Damage impacts and failure modes on a second and third span of an RC skew highway girder bridge under surface explosion using FEM-SPH coupling and non-explosive reactive armour, *Int. J. Protect. Struct*. (2025) 20414196251326186.
[29] B. Zhou, X. Chen, S. Chen, Failure mechanism and residual load-bearing capacity of blast-loaded reinforced concrete bridge column considering bottom corrosion effect, *Struct*. **75** (2025) 108668.
[30] Z. Wu, Y. Zheng, W. Wang, C. Zhou, L. Chen, H. Xiang, H. Fang, Dynamic performance of prestressed ECC-concrete composite T-beam bridge subjected to close-in blast loading, *Case Stud. Constr. Mater*. **22** (2025) e04992.
[31] A. Bagherzadeh Azar, A. Sari, Failure analysis and structural resilience of a masonry arch bridge subjected to blast loads: the case study, Halilviran Bridge, *Mech. Adv. Mater. Struct*. **32** (2025) 4041–4064.
[32] Y. Mi, H. Ren, C. Sun, J. Zhao, W. Wang, Z. Yang, Y. Chen, Dynamic behavior and residual performance of CFDSTCs under coupled collision and blast loads, *Case Stud. Constr. Mater*. **22** (2025) e04147.
[33] A. Alsendi, C.D. Eamon, Quantitative resistance assessment of steel girder bridges subjected to blast loads, *J. Bridge Eng*. **29** (2024) 04024069.
[34] L. Zhang et al., Dynamic response and damage assessment of steel box girder bridge under far-field blast loading, *Adv. Struct. Eng*. (2024) 13694332251344646.
[35] L. Gan et al., Experimental and numerical study of damage mechanism of steel box girders under external blast loads, *J. Constr. Steel Res*. **198** (2022) 107578.
[36] S. Yuan, H. Hao, Z. Zong, J. Li, Numerical analysis of axial load effects on RC bridge columns under blast loading, *Adv. Struct. Eng*. **24** (2021) 1399–1414.
[37] K. Patel, A. Goswami, S.D. Adhikary, Response characterization of highway bridge piers subjected to blast loading, *Struct. Concr*. **21** (2020) 2377–2395.
[38] R. Mudragada, S.S. Mishra, Effect of blast loading and resulting progressive failure of a cable-stayed bridge, *SN Appl. Sci*. **3** (2021) 322.
[39] R.U.N. Dar, M. Alam, Damage evaluation of a reinforced concrete bridge subjected to blast loading, in: Recent Advances in Structural Engineering: Select Proceedings of NCRASE 2020, Springer, Singapore (2021) pp. 131–142.
[40] S.K. Hashemi, M.A. Bradford, H.R. Valipour, Dynamic response of cable-stayed bridge under blast load, *Eng. Struct*. **127** (2016) 719–736.
[41] Y. Li, S. He, Research of steel-concrete composite bridge under blasting loads, *Adv. Civ. Eng*. **2018** (2018) 5748278.
[42] Z. Zhu, Y. Li, C. Ma, Damage analysis of small box girder bridges under a car explosion, *Eng. Fail. Anal*. **120** (2021) 105104.
[43] C.D. Tetougueni, P. Zampieri, C. Pellegrino, Structural performance of a steel cable-stayed bridge under blast loading considering different stay patterns, *Eng. Struct*. **219** (2020) 110739.
[44] C.D. Tetougueni, P. Zampieri, Structural response of cable-stayed bridge subjected to blast load, *Procedia Struct. Integr*. **18** (2019) 765–774.
[45] W. Chen, H. Hao, S. Chen, Numerical analysis of prestressed reinforced concrete beam subjected to blast loading, *Mater. Des*. **65** (2015) 662–674.
[46] L. Zhang, H. Hao, Dynamic response and damage of bridge structures subjected to blast loads, *Int. J. Impact Eng*. (2015).